Protection against maternal infection-associated fetal growth restriction: proof-of-concept with a microbial-derived immunomodulator

NM Scott[1,5], JF Lauzon-Joset[1,5], AC Jones[1], KT Mincham[1], NM Troy[1], J Leffler[1], M Serralha[1], SL Prescott[1,2], SA Robertson[3], C Pasquali[4], A Bosco[1,6], PG Holt[1,6] and DH Strickland[1,6]

Infection-associated inflammatory stress during pregnancy is the most common cause of fetal growth restriction and/or miscarriage. Treatment strategies for protection of at-risk mothers are limited to a narrow range of vaccines, which do not cover the bulk of the common pathogens most frequently encountered. Using mouse models, we demonstrate that oral treatment during pregnancy with a microbial-derived immunomodulator (OM85), currently used clinically for attenuation of infection-associated airway inflammatory symptoms in infants–adults, markedly reduces risk for fetal loss/growth restriction resulting from maternal challenge with bacterial lipopolysaccharide or influenza. Focusing on LPS exposure, we demonstrate that the key molecular indices of maternal inflammatory stress, notably high levels of RANTES, MIP-1α, CCL2, KC, and G-CSF (granulocyte colony-stimulating factor) in gestational tissues/serum, are abrogated by OM85 pretreatment. Systems-level analyses conducted in parallel using RNASeq revealed that OM85 pretreatment selectively tunes LPS-induced activation in maternal gestational tissues for attenuated expression of TNF, IL1, and IFNG-driven proinflammatory networks, without constraining Type1-IFN-associated networks central to first-line antimicrobial defense. This study suggests that broad-spectrum protection-of-pregnancy against infection-associated inflammatory stress, without compromising capacity for efficient pathogen eradication, represents an achievable therapeutic goal.

INTRODUCTION

Systemic inflammatory processes triggered by infections during pregnancy can have adverse short-term effects on maternal well-being,[1,2] and can additionally negatively impact on ensuing fetal growth and survival via disturbance of immune homeostatic processes in gestational tissues.[3,4] Moreover, intrauterine growth restriction following maternal infection is also associated with increased disease risk postnatally in surviving fetuses. It is now widely recognized that multiple (including common) pathogens, as well as fetal growth restriction regardless of cause, constitutes a risk factor for the development of a range of chronic diseases in later life.[5,6] With respect to risk associated specifically with infections, maternal immunization represents the only protective treatment option currently available,[7] but the breadth of potential coverage against the wide range of common pathogens potentially encountered during pregnancy is severely limited by vaccine availability.

To address this latter limitation, we have turned to an alternative concept, notably the potential use of immunomodulator(s) to boost the capacity of the maternal immune system to efficiently clear infections, a capacity that is known to be compromised during pregnancy.[1,2] For this purpose, we have turned to an orally delivered microbial-derived immunomodulatory agent OM85. This agent comprises a standardized lyophilized extract of a mixture of major respiratory bacterial

pathogens containing *Haemophilus influenzae, Streptococcus (Diplococcus) pneumoniae, Klebsiella pneumoniae ssp. pneumoniae et ssp. ozaenae, Staphylococcus aureus, Streptococcus pyogenes et sanguinis (viridans), Moraxella (Branhamella/ Neisseria) catarrhalis,* and includes multiple TLR ligands.[8,9] OM85 has a well-established clinical safety profile spanning a period dating back to the 1980s, including in infants as young as 6 months.[10–12] In independent randomized clinical trials, OM85 has previously been shown to attenuate infection-associated inflammatory symptoms in infants[13,14] and adults[15] with predisposition to recurrent viral and/or bacterial infections. By extension, we hypothesized that prophylactic treatment during pregnancy could potentially provide broad-spectrum protection to mitigate the known downstream effects of microbial pathogens in general on pregnancy outcomes, and in the present study we have sought proof-of-concept and associated mode-of-action data in a mouse model.

RESULTS
Protection against exaggerated responses to influenza infection during pregnancy
We used a model utilizing the Influenza A/H1N1/PR8 (PR8) murine strain[16] (**Supplementary Figure 1**) to investigate the effects of OM85 pretreatment on the ensuing effects of live PR8 infection on gestation day (GD) 9.5 during pregnancy. In humans, pregnancy has been associated with a predisposition to Influenza A infection and heightened disease severity.[2,17,18] A comparable pattern was clearly evident in infected pregnant mice 8 days after infection with PR8 with increased levels of viral replication in lung tissue (**Supplementary Figure 2a**), which was associated with higher clinical distress scores (**Supplementary Figure 2b**) and proportionately higher weight loss (**Supplementary Figure 2c**) over the disease course relative to comparably infected non-pregnant mice.

To evaluate the capacity of OM85 to protect against these effects in pregnant mice, a series of animals were pretreated with OM85 or placebo for 8 consecutive days from vaginal plug detection (GD0.5) until the day preceding infection (GD8.5). Maternal clinical data were collected daily until killing at GD17.5, and as illustrated in **Figure 1a**, OM85 pretreatment reduced clinical stress scores from GD14.5 onwards, but did not significantly modify infection-associated weight loss (**Figure 1b**). An additional series of assessments were performed at GD17.5, including cellular profiling of broncho-alveolar (BAL) washouts, PCR quantification of viral copy numbers in lung tissue homogenates, and fetal/placental weights measured. These data together with outcome day maternal weight and clinical scores, were integrated via Principal Component Analysis[19] as summarized in **Figure 1c** and **Supplementary Table 1**, which identified two clusters within the OM-treated group. One of these (cluster A) clearly demonstrated attenuated severity of infection-related outcomes (maternal and fetal) with a response phenotype that falls between non-infected controls and the PR8-infected/ untreated animals. The second cluster (B) did not demonstrate any overall effect of OM85 pretreatment on the response to

infection and data remain overlapped with the PR8-infected/ non-treated group in the principal component analysis (PCA). This heterogeneity of OM85 responder phenotypes suggested that the treatment regimen (which comprised pre-infection dosing only for the experiments described above) may have been suboptimal. By extending OM85 treatment to additionally include the period of infection (i.e., continuous treatment from GD0.5 to GD16.5), the clinical stress scores and maternal weight trajectories over the time course now corresponded to those of OM85 responder group A (i.e., attenuated disease) in approximately 90% of animals (**Supplementary Figure 3**). Focusing specifically on clinical parameters on GD17.5, it is evident that daily treatment significantly reduced infection-mediated clinical stress (**Figure 1d**), fetal weight loss (**Figure 1e**), and viral titers in lung tissue (**Figure 1f**).

Protection of pregnancy against the toxic effects of bacterial LPS challenge
We next used a rigorously validated LPS exposure model[20,21] to mimic bacterial infection during pregnancy and evaluated the potential of OM85, administered daily from GD9.5 until just before LPS administration on GD16.5 (**Supplementary Figure 4**), to attenuate LPS-induced fetal resorption and/or growth restriction over the ensuing 24 h. The dose of LPS used in this study (10 µg) was selected to result in approximately 50% fetal loss with significant weight reduction (mean 13%) in surviving pups compared with those from control pregnant mice (**Supplementary Figure 5a,b** and **Figure 2a,b**), thus allowing for sufficient viable fetal tissues for further analyses and the potential to identify significant differences in the fetal weights. Pretreatment of pregnant mice with OM85 before LPS administration resulted in significantly improved fetal survival rates (**Figure 2a**) and prevention of fetal weight loss (**Figure 2b**) compared with LPS-injected control pregnant mice. The analyses in **Figure 2b** utilized data only from pregnant mice with a litter size of 7 across all the groups of mice, thereby eliminating litter size as a confounder in analyses relating to fetal weight loss; however, importantly, comparable findings were obtained across the collective study when all the litters were included (**Supplementary Figure 5c**). We did not observe any significant changes in placenta weight across any of the groups of mice regardless of OM85 treatment or LPS injection (data not shown). However, as expected due to the differences in fetal weight, the fetal:placenta weight ratio was significantly different between treatment groups (data not shown).

Modulation of infection-associated immune cell trafficking in gestational tissues during pregnancy
Using the LPS model, we next proceeded to studies on the effects of OM85 treatment during pregnancy on immune cell populations known to have important roles in the maintenance of immunological homeostasis in gestational tissues[22–25], using multi-parameter flow cytometry (detailed in the 'Methods' section and panels shown in **Supplementary Table 2**). Manual gating was also confirmed using algorithm-based gating strategies (viSNE; data not shown). The gestational tissues
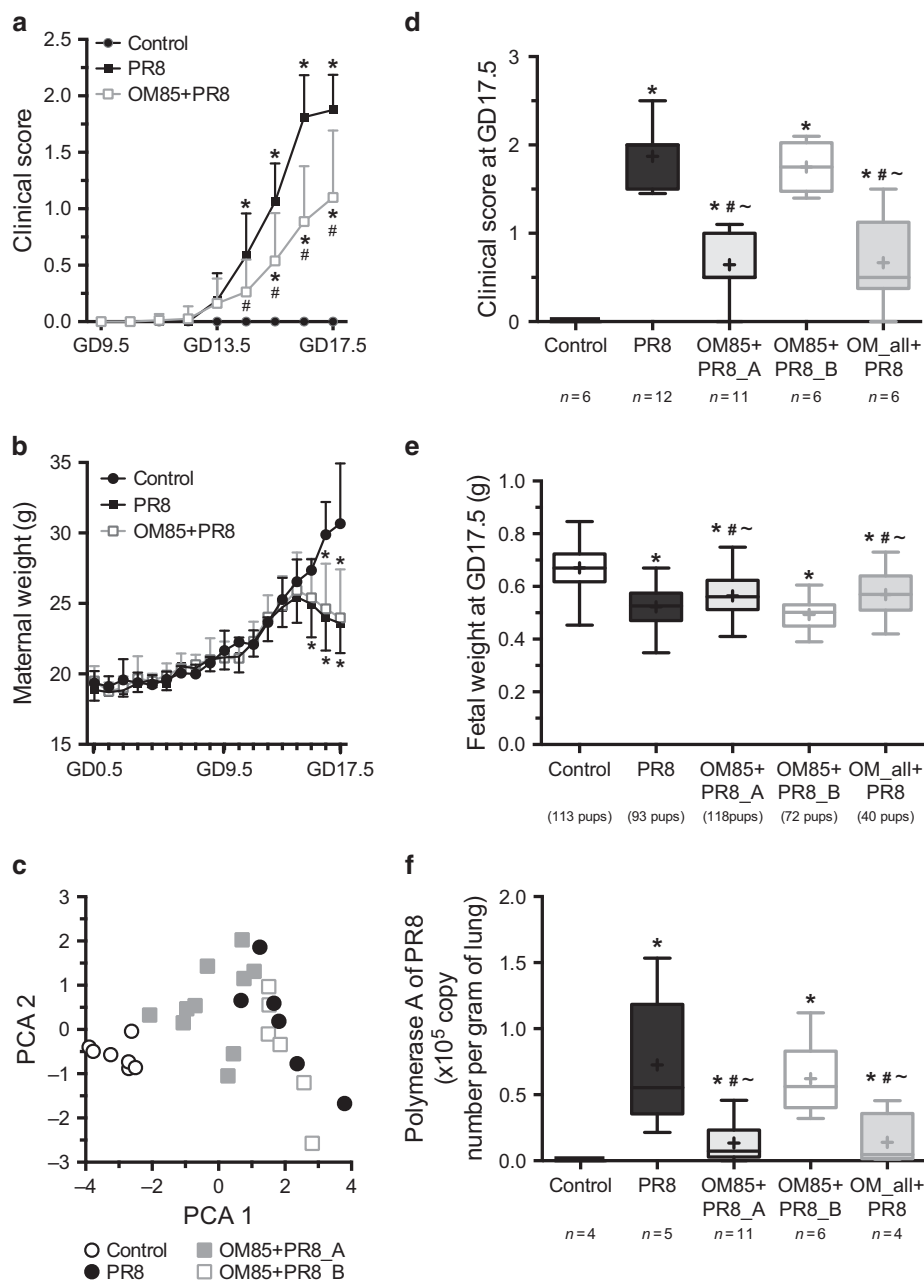
Figure 1 OM85 reduces the severity of Influenza infection in pregnant mice. (**a**) Clinical score and (**b**) maternal weight of control non-pregnant mice vs. timed mated mice infected with PR8 with or without OM85 pretreatment from gestation day (GD) 0.5 to GD8.5. Data from mice treated with OM85 alone were not different from the control group; (control, $n = 6$; PR8, $n = 12$; OM85 + PR8, $n = 20$; collected from >5 independent experiments). Data are displayed as mean ± s.d. Statistical analysis was done by two-way analysis of variance (ANOVA) with Bonferroni multiple-comparison test; *$P < 0.05$ vs. control, #$P < 0.05$ vs. PR8. (**c**) Principal component analysis (PCA) using the parameters described in **Supplementary Table 1**; (control, $n = 6$; PR8, $n = 6$; OM85 + PR8_A, $n = 10$; OM85 + PR8_B, $n = 6$; collected from >5 independent experiments). (**d–f**) PR8 infection of mice pretreated with OM85 from GD0.5 until GD8.5 (OM85 + PR8) or during the whole pregnancy (OM_all + PR8, $n = 6$). At GD17.5, clinical score (**d**), fetal weights (**e**), and lung viral load (**f**) (measured in lung homogenate by quantitative PCR) were assessed. The viral load of the controls was below the detection limit of the assay. Statistical analysis was done by one-way ANOVA with Bonferroni's multiple-comparison test; *$P < 0.05$ vs. control, #$P < 0.05$ vs. PR8, ~$P < 0.05$ vs. OM85 + PR8_B.

analyzed are referred to in the text as placenta, uterus, decidua (see the 'Methods' section and **Supplementary Figure 4** for a more detailed description of precise tissue collection methodology), and draining lymph nodes (para-aortic lymph node). Total CD45^{+} cell yields were not

significantly influenced by LPS exposure (data not shown). Among the CD45^{+} cells, the functions of several subpopulations are known to be critically important to successful pregnancy[23] and LPS induced occasional proportional changes for total myeloid, T-cell, B-cell, and macrophage
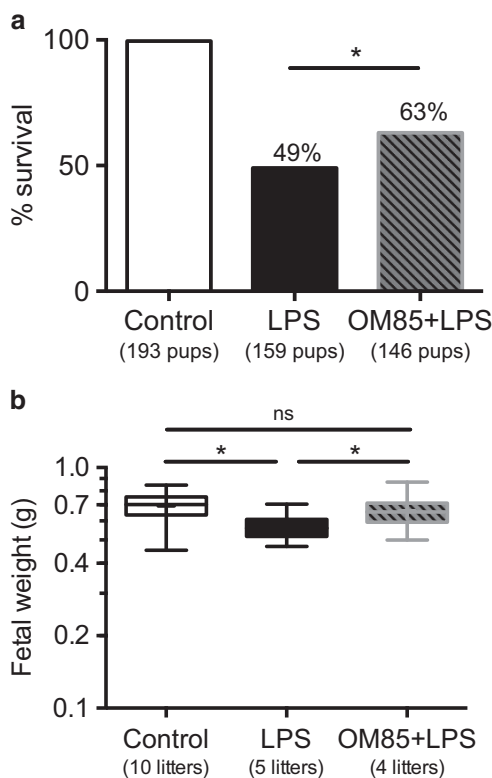
Figure 2 OM85 treatment before maternal LPS exposure protects against adverse pregnancy outcomes. (**a**) Percent survival of offspring from all litters size (with $n > 25$ litters per group, total pup number per group shown in parentheses). Statistical analysis was done by Chi-squared test; *$P < 0.05$. (**b**) Time-mated mice were pretreated or not with OM85 and injected with LPS at gestation day (GD) 16.5. At GD17.5, fetal weights were measured. Data shown are mean ± s.d. for litter size of seven pups (derived from the same animals as per **a**). Statistical analysis was done by one-way analysis of variance (ANOVA) with Bonferroni multiple-comparison test; *$P < 0.05$, NS, not significantly different.

populations in the tissues examined, but these were not modified by OM85 pretreatment (**Supplementary Figure 6**). However, as illustrated in **Figure 3**, the profile of the cellular response to LPS exposure in animals pretreated with OM85 was notably different for four rare immunomodulatory cell populations: T-regulatory (Treg), plasmacytoid dendritic cells (pDCs), conventional DCs (cDCs), and myeloid derived suppressor cells (MDSC). In our model, LPS drives marked accumulation of MDSCs in uterus/placenta (**Figure 3a,b**) and Tregs in uterus/decidua (**Figure 3a,c**). Induction of this inflammatory cellular response was attenuated in OM85-pretreated pregnant mice; dysregulation of MDSC at the fetomaternal interface has been associated with poor pregnancy outcomes.[26] In contrast, LPS exposure depleted resident uterine/placental cDC populations (**Figure 3a,b**), likely by stimulating their migration to draining para-aortic lymph node (**Figure 3d**), and this was also attenuated by OM85. Moreover, the LPS-induced upregulation of activation markers CD40 and CD86 on cDCs in gestational tissues was conserved and/or enhanced by OM85 (**Supplementary Figure 7**). It is pertinent to note in this regard that entrapment of functional cDCs in gestational

tissues has been linked to regulatory processes that contribute to successful pregnancy outcomes.[27] It is additionally evident that recruitment of pDCs into uterus/decidua by LPS is significantly enhanced by OM85 pretreatment (further discussion below).

Attenuation of infection-associated inflammatory mediator production in gestational tissues

As measures of maternal inflammatory stress, we next determined at the time of killing on GD17.5 levels of a broad array of cytokines in maternal serum (**Supplementary Figure 8**) and uterine tissue (**Supplementary Figure 9**; comparable data were obtained for the placenta—not shown). The largest and most consistent changes induced by LPS involved RANTES, MIP-1α, KC, CCL2, and G-CSF (granulocyte colony-stimulating factor) production (**Figure 4**). Of note, the production of these pro-inflammatory mediators in response to LPS was considerably reduced in pregnant mice that were pretreated with OM85 (**Figure 4a–c** for uterus, placenta, and maternal serum, respectively). The observation that some but not all pro-inflammatory cytokines were attenuated at the protein level suggested a degree of selectivity in the action of OM85 pretreatment in orchestrating the direction of the immune response to LPS. To explore this finding in more detail at the systems level, we used RNASeq profiling of maternal tissues.

Systems-level analyses targeting mechanism of action of OM85

To decipher the molecular mechanisms that underpin OM85-mediated reprogramming of the LPS response, we identified differentially expressed genes and networks[28,29] from RNASeq profiles of the uterus (using portions of same samples analyzed for cytokine levels and cellular profiling) and decidua (obtained from independent animals from each group). These data were further interrogated with upstream regulator analysis[30] to identify the molecular drivers of the responses (detailed in the 'Methods' section). LPS challenge induced a strong perturbation of the gene expression program in decidua and uterus compared with control (non LPS-exposed) pregnant mice. Specifically, in the order of 3,000 differentially expressed genes (DEGs) were identified in each tissue (false discovery rate (FDR) < 0.05; decidua: 2,855 genes (**Figure 5a** and **Supplementary Table 3**) and uterus: 2,877 genes (**Supplementary Figure 10a** and **Supplementary Table 4**)), and subsequent pathways analyses using InnateDB clearly identified a series of LPS-sensitive innate and adaptive immunoinflammatory pathways in both tissues (decidua: P values 1×10^{-3}–1.2×10^{-21} (**Supplementary Table 5**) and uterus: P values 1.71×10^{-2}–5.93×10^{-19} (**Supplementary Table 6**)).

Parallel analyses comparing gene expression in LPS-challenged OM85-pretreated pregnant mice to controls revealed a marked decrease in the number of genes induced by LPS, with 762 DEGs identified in decidua (FDR < 0.05, **Figure 5b**, **Supplementary Table 7**) and 709 DEGs in uterus (**Supplementary Figure 10b**, **Supplementary Table 8**),
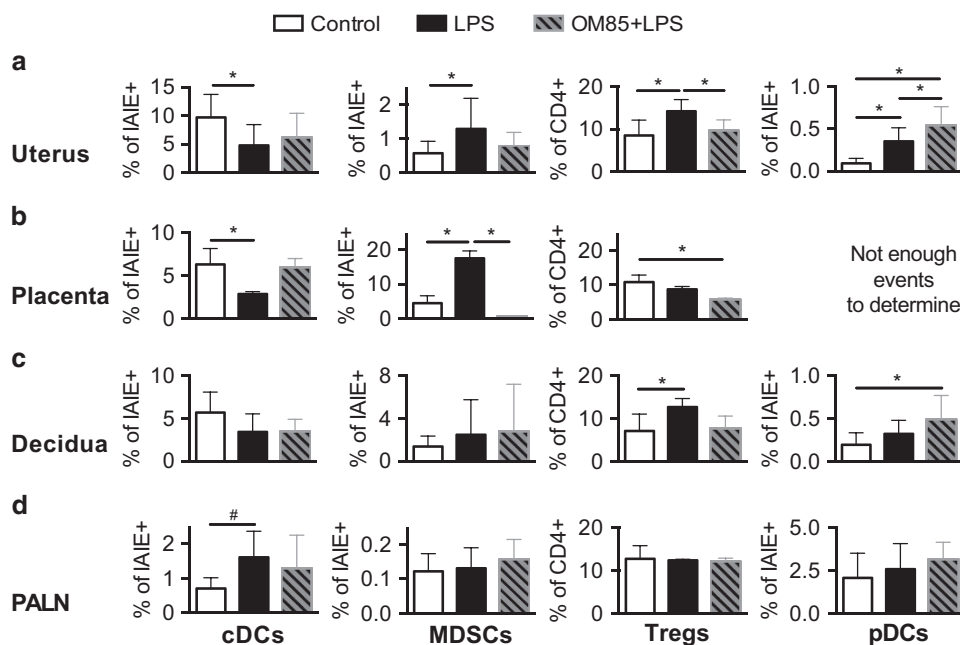
Figure 3 OM85 pretreatment modulates the inflammatory immune cell response to maternal lipopolysaccharide (LPS) exposure. Single-cell suspensions prepared from (**a**) uterus, (**b**) placenta, (**c**) decidua, and (**d**) para-aortic lymph node (PALN) tissues collected from control pregnant vs. LPS-exposed pregnant mice with and without OM85 pretreatment, were analyzed via flow cytometry for conventional dendritic cells (cDCs) (CD45$^+$F480$^-$ I-A/I-E$^+$Ly6G/C$^-$B220$^-$CD11c$^+$), myeloid derived suppressor cells (MDSCs) (CD45$^+$F480$^-$I-A/I-E$^+$Ly6G/C$^+$B220$^-$CD11c$^-$), T regulatory (Tregs) (CD45$^+$CD3$^+$CD4$^+$CD8$^-$CD25$^+$FoxP3$^+$), and plasmacytoid DCs (pDCs) (CD45$^+$F480$^-$I-A/I-E$^+$Ly6G/C$^+$B220$^+$CD11b$^-$CD11c^{lo}). Data displayed as mean ± s.d., $n = 7$ per group collected from > 5 independent experiments. Statistical analysis was done by one-way analysis of variance (ANOVA) with Bonferroni multiple-comparison test (*$P < 0.05$) or by unpaired t-test ($^\#P < 0.05$).

respectively, but the overall spectrum of underlying LPS-sensitive immunoinflammatory pathways (decidua: P values 1×10^{-7}–7×10^{-28}, (**Supplementary Table 9**) and uterus: P values 1.1×10^{-3}–1×10^{-25} (**Supplementary Table 10**)) was qualitatively similar to that seen above in tissues from non-treated animals. However, a direct comparison between LPS-challenged mice with vs. without OM85 pretreatment highlighted significant treatment-associated attenuation of multiple inflammation-associated genes in these tissues (global responses in **Figure 5c**, **Supplementary Figure 10c** and **Supplementary Tables 11/12**; exemplary genes in **Supplementary Figure 11**).

Next, we used upstream regulator analysis to identify the putative molecular drivers of the observed differential gene expression patterns. These analyses confirmed LPS itself as the most significant driver of the LPS response (**Figure 5a**), demonstrating the overall plausibility of this model with the published LPS literature. At the top of the rank order of subsequent drivers of the LPS response were TNF, IFNG, IL1B, and IL6, which respectively accounted for 422, 367, 250, and 196 of the differentially expressed genes in the decidua. Similarly, in the uterus, we identified IFNG, TNF, IL1B, and IL6 as the most significant drivers of the LPS response, which respectively accounted for 390, 428, 264, 206 of the differentially expressed genes (**Supplementary Figure 10a**). Consistent with reduced inflammatory responses to LPS in mice pretreated with OM85, the number of genes for the same

drivers was dramatically reduced in the decidua (TNF: 152, IFNG: 179, IL1B: 114, and IL6: 89; **Figure 5b**) and in the uterus (IFNG: 192, TNF: 154, IL1B: 110, IL6: 86; **Supplementary Figure 10b**). However, it is noteworthy that in the decidua and the uterus of OM85 pretreated mice, genes from the type I interferon pathway were enriched amongst the top of the rank order of molecular drivers (IFNAR1, IRF7, IFNA, IFNB; **Figure 5b** and **Supplementary Figure 10b**), whereas proinflammatory drivers (TNF, IL1B, IL6) in general had lower ranks. Last, we identified the molecular drivers of the differential response to LPS challenge in mice with vs. without OM85 pretreatment. The data showed that the expression of multiple proinflammatory pathways (IL1B, TNF, IFNG, and IL6; **Figure 5c**) was decreased in the decidua of OM85 pretreated mice after LPS challenge in comparison with LPS-treated control pregnant mice. We observed similar patterns of attenuated inflammatory gene expression programs in the uterus (IFNG, TNF, IL1B, and IL6, **Supplementary Figure 10c**).

We used coexpression network analysis to provide a holistic view of the gene expression program in decidua and uterus, focusing on the most variables genes. In the decidua, the resulting network contained 4,271 genes organized into 17 coexpression modules (labeled A–Q; **Supplementary Figure 12a** and **Figure 6**). LPS challenge modulated the expression of seven modules (modules A, D, E, F, H, J, and Q; median FDR < 0.05, **Figure 6a**). In contrast, if the mice were
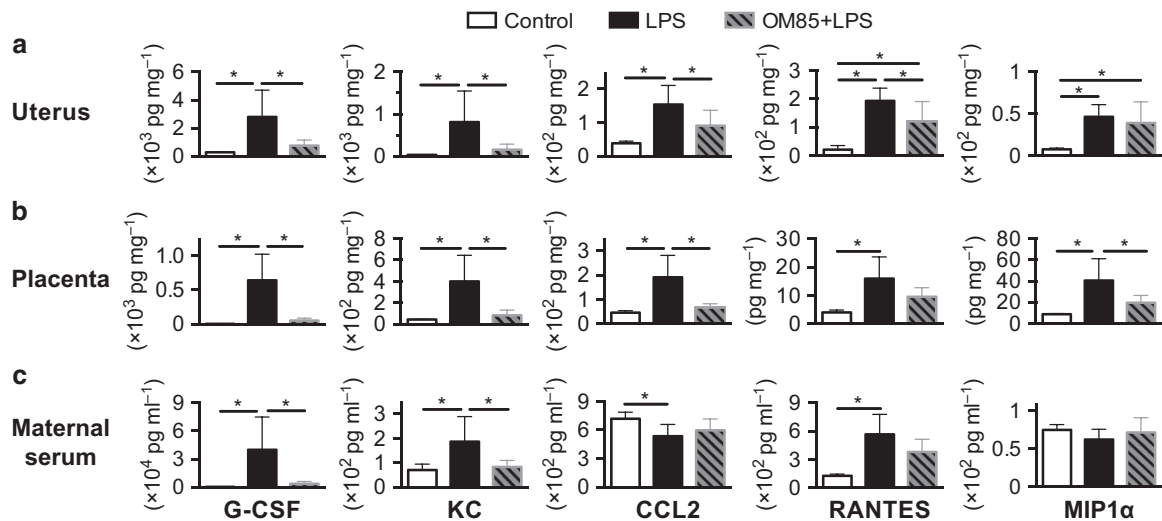
Figure 4 OM85 pretreatment before maternal lipopolysaccharide (LPS) exposure attenuates the inflammatory cytokine response. Protein extracted from (**a**) uterus, (**b**) placenta, and (**c**) maternal serum collected at gestation day (GD) 17.5 from control pregnant vs. LPS exposed pregnant mice with and without OM85 pretreatment was used to determine tissue cytokine profiles. Shown are the levels of G-CSF, KC, CCL2, RANTES, and MIP1α as assessed by multiplex cytokine analysis. Data displayed as mean $\pm$ s.d., $n = 5$–6 per group collected from >3 independent experiments. Statistical analysis was done by one-way analysis of variance (ANOVA) with Bonferroni multiple-comparison test; $*P < 0.05$.

pretreated with OM85, only two modules were perturbed by LPS challenge (modules A and F; median FDR < 0.01, **Figure 6b**). In the uterus, the LPS-induced coexpression network comprised 4,185 genes structured into 11 coexpression modules (**Supplementary Figure 12b**). LPS challenge perturbed the expression of four modules (B, I, J, and K; FDR < 0.05, **Supplementary Figure 12c**), but only one of these modules was modulated by LPS in mice pretreated with OM85 (module B; median FDR < 0.01, **Supplementary Figure 12d**). Last, we characterized the upstream regulators that coordinated the effect of each differentially expressed module (**Figure 7**). In decidua, the LPS response was largely driven by proinflammatory pathways (e.g., OSM, TNF, IL1B, CEBPB, NFKB, MyD88, module E, module J, module Q; **Figure 7a**). OM85 pretreatment silenced the proinflammatory upstream regulators while conserving the modules driven by IRF7 (module A) and IFNG (module F; **Figure 7b**). Similar effects were seen in the uterus, upstream regulator analysis suggested that module B was driven by IFNG and IRF7 (data not shown). Again, OM85 pretreatment silenced modules associated with proinflammatory pathways (e.g., TNF, IL1B, IL6, NFKB), but not type I IFN response pathways (data not shown). These data show that OM85 pretreatment preferentially attenuates proinflammatory gene networks, but preserves interferon-mediated networks.

Safety profile of OM85 during normal pregnancy

In conjunction with the functional studies detailed above relating to OM85 use as an anti-inflammatory agent, we additionally evaluated the effects of prophylactic treatment with OM85 during gestation on normal pregnancy outcomes in the absence of infectious challenge. RNASeq analyses demonstrated that groups of pregnant mice exposed only to OM85

treatment for 8 days from GD9.5 (as per LPS model) induced a very limited perturbation of the gene expression program with only 15 and 1 DEGs seen in the decidua and uterus, respectively (data not shown). In terms of cellular composition within gestational tissues, the proportions of the immune cell populations including NK cells, cDC, pDC, B cells, T regulatory cells, MDSC, and other myeloid populations were unchanged by OM85 treatment (data not shown), with the exception of small but significant increases in frequency of macrophages and T-cells in the placenta only (data not shown). OM85 treatment did not skew the cytokine milieu across the range of Th1, Th2, proinflammatory, and regulatory cytokines measured in the maternal serum, uterus, and placental tissue (data not shown). On average, OM85 decreased cytokines in the maternal serum by 20%, the uterus tissue by 5%, and increased cytokines in the placental tissue by an average of 36% (data not shown).

Groups of control pregnant mice vs. those treated for 8 days from GD 9.5 with OM85 (as per the LPS model) had similar weight gain curves (**Figure 8a**) and litter sizes (**Figure 8b**). In addition, there were no significant differences in the mean pup birth weight or growth trajectory (**Figure 8c**); fetal or placenta weight or fetal:placenta weight ratio at GD17.5 (**Supplementary Figure 13a,b,c**, respectively). Further, we did not find any differences at GD17.5 in the number of viable implantations per pregnant mouse, gestational time to parturition, number of resorptions per pregnant mouse (**Supplementary Figure 13d,e,f**, respectively) between groups of control vs. treated pregnant mice. In separate experiments, we also determined the safety of OM85 given over the first 8 days from detection of plug as per the influenza model on the clinical outcomes of pregnancy and as above found no changes (data not shown). Collectively, across maternal and fetal clinical parameters, immune cell and molecular profiling, our data
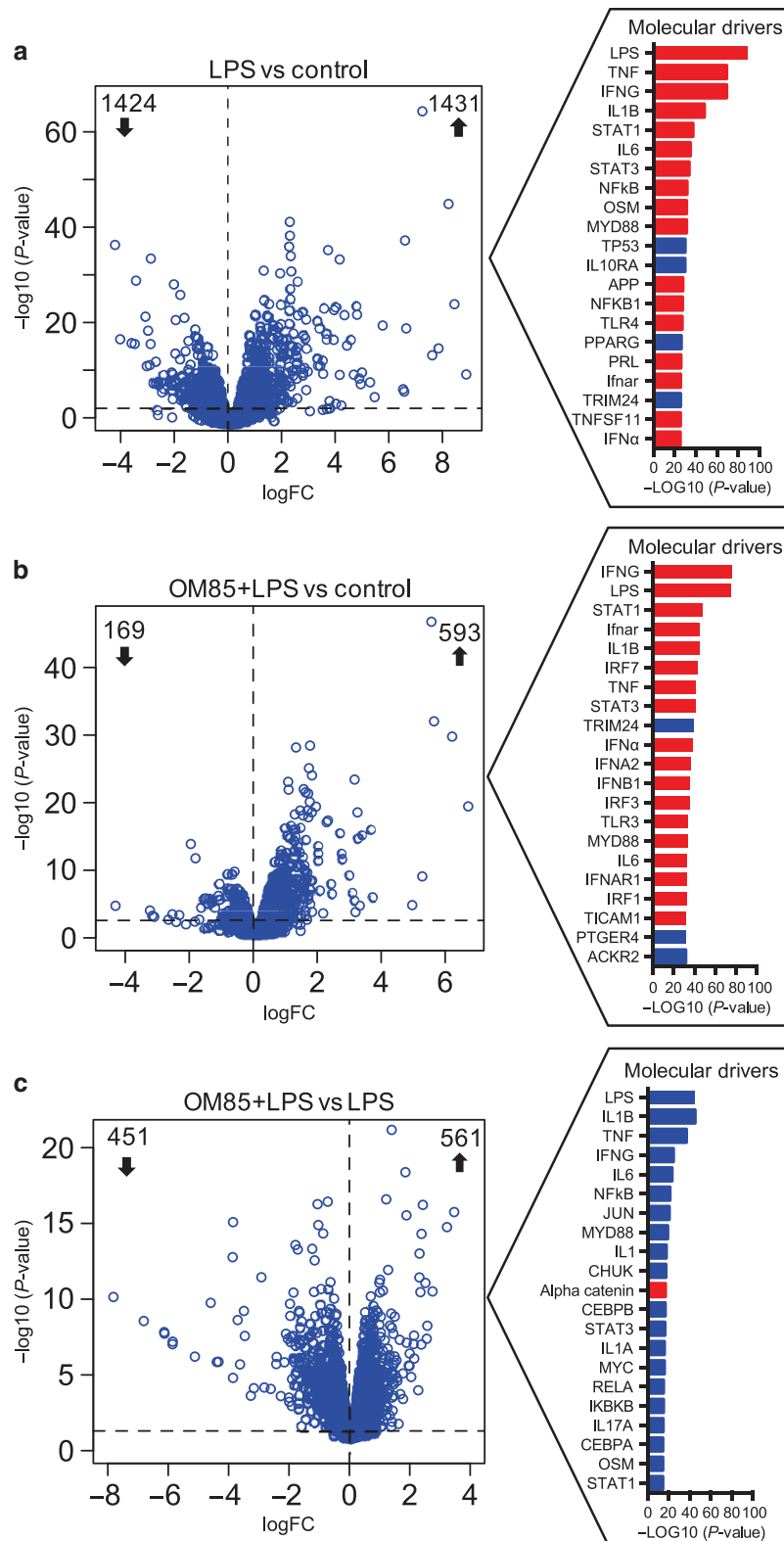
Figure 5 OM85 pretreatment before maternal lipopolysaccharide (LPS) exposure attenuates inflammatory gene programs in decidua. Left panels: differentially expressed genes were identified using edgeR in decidua from (**a**) LPS-challenged vs. control pregnant mice; (**b**) OM85-pretreated LPS-challenged vs. control pregnant mice; (**c**) OM85-pretreated LPS-challenged vs. LPS-challenged pregnant mice. Data are mean, $n = 5$ per group collected from > 3 independent experiments. The dashed horizontal lines indicate a false discovery rate (FDR) < 0.05. Right panels: molecular drivers of the differential expression patterns were identified using Upstream Regulator Analysis. Driver genes shown in red were activated and those shown in blue were inhibited (all drivers had absolute activation Z-scores > 2.0).
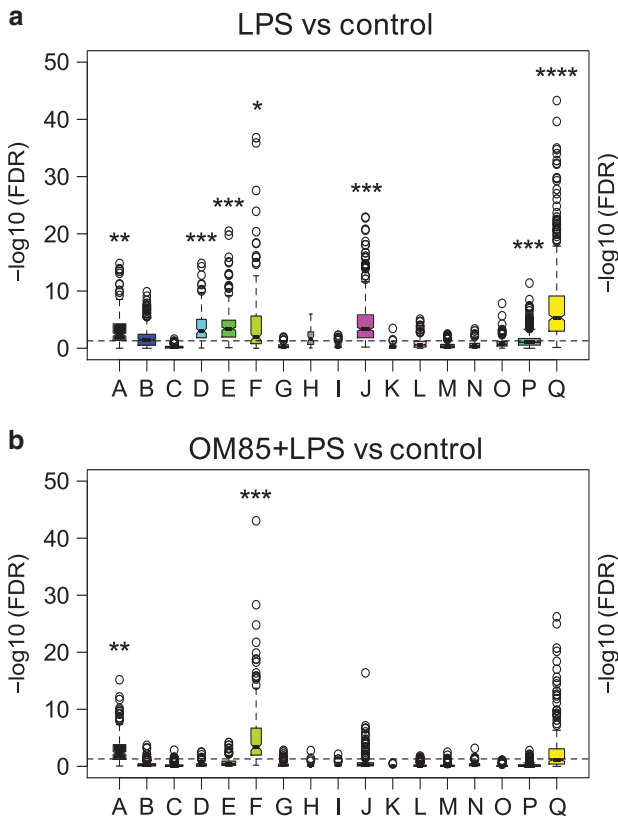
Figure 6 OM85 pretreatment modulates expression of inflammatory gene coexpression networks in decidua and uterus following maternal lipopolysaccharide (LPS) exposure. Network analysis (WGCNA) was performed on gene expression patterns focusing on the most variable genes to identify the coexpression network. The overall expression of the modules in decidua was compared in LPS-challenged vs. control pregnant mice (**a**) and in OM85-pretreated LPS-challenged vs. control pregnant mice (**b**). The *P* values were derived from an edgeR analysis and the dashed horizontal lines indicate a false discovery rate (FDR) <0.05. ****: median FDR <0.0001; ***: median FDR <0.001; **: median FDR <0.01; *: median FDR <0.05.

provide supporting evidence that OM85 can be safely used during gestation.

DISCUSSION

Immune function(s) in gestational tissues require fine control to balance the conflicting needs of suppression of maternal responses against fetal allograft antigens, while enabling effective defense against microbial pathogens. An additional imperative is that maternal expression of antimicrobial immunity, particularly elements of these responses that have potential to spill over into the systemic compartment, must be tightly regulated to limit the risk of "bystander" inflammatory damage to the highly vascularized tissues at the fetomaternal interface. However this balance is frequently not achieved, and indeed heightening of infection susceptibility and accompanying symptomatology is a recognized feature of the normal pregnant state.[2,24,31] This infection-susceptible phenotype is additionally a common feature of infancy, a hallmark of which is the severe lower respiratory tract infections that peak in frequency within the first year of life.[32,33] Recent clinical studies

suggest that prophylactic treatment of infants with the microbial-derived immunomodulatory agent OM85 can significantly attenuate the intensity and duration of their respiratory infection-associated symptoms.[10–14] We posited that by extension, this same agent may offer similar protection during pregnancy, and if so this may also mitigate the known downstream effects of maternal infection on fetal growth restriction and/or loss.

Using a model of live Influenza A infection with an inoculum that permitted 100% survival of pups over the ensuing 8 days, preventive treatment with OM85 resulted in a dose-dependent enhancement of viral clearance in infected pregnant mice, significantly reduced maternal clinical stress scores across the infection time course, and attenuated the infection-associated inhibition of fetal growth rates, as shown in **Figure 1**/**Supplementary Figure 3**. Interestingly, maximal response was observed when the treatment was given both before and during the infection, suggesting that the cumulative dose of OM85 is important to train the immune system adequately.

OM85 pretreatment also provides significant protection, as illustrated in **Figure 2**, against the effects of maternal bacterial LPS exposure on subsequent acute fetal loss and/or growth restriction. Mechanistic studies focusing on the LPS model to characterize the nature of the changes induced by OM85 pretreatment in association with protection against the toxic effects of LPS revealed the capacity of OM85 to fine tune the immune response. Systems-level analyses of RNASeq profiles from maternal gestational tissues provided a global view of the underlying gene networks involved. This demonstrated that LPS exposure of control pregnant mice perturbed around 3,000 genes in the decidua and uterus, which was markedly reduced in mice pretreated with OM85 to around 700 genes. Upstream regulator analysis suggested that the LPS response was mainly driven by TNF, IL1B, IL6, and IFNs, and OM85 pretreatment selectively attenuated the activation of proinflammatory pathways (TNF, IL1B, IL6) while the interferon response pathway (IRF7, IFNG)[34–36] was preserved. It is noteworthy that TNF, IL1, and IL6 are prominent among the list of inflammatory mediators that are recognized contributors to pregnancy loss/complications[37,38] and accordingly selective suppression of their production while concomitantly conserving type 1 IFN pathways that are central to antimicrobial defense, provides a plausible explanation for the pregnancy sparing effects of OM85 pretreatment in the face of microbial challenge.

The precise molecular mechanism(s) through which OM85 regulates the balance between these inflammatory and microbial defense pathways following LPS binding remains to be determined. A precedent for differential regulation of these two pathways can be found in recent literature demonstrating that LPS triggering can sequentially activate two distinct signaling pathways, via plasma membrane-localized and endosomal TLR4/LPS complexes.[35,39] The former induces TIRAP–MyD88 signaling while the latter induces TRAM–TRIF signaling, resulting respectively in the production of pro-inflammatory cytokines and type 1 IFNs. On this basis, it is feasible that one consequence of OM85 treatment may be to alter the balance
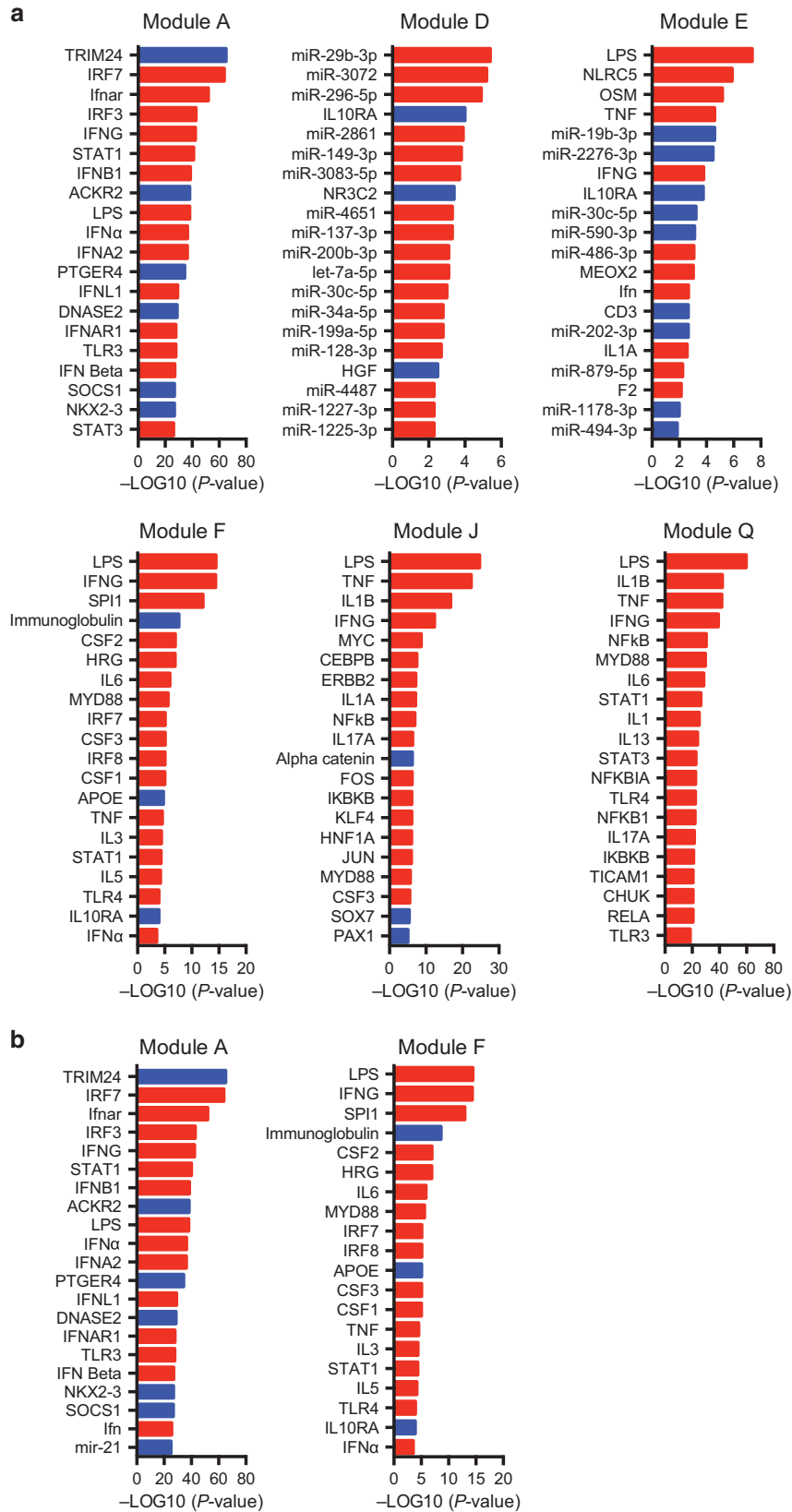
Figure 7 Molecular drivers of gene coexpression modules in decidua from lipopolysaccharide (LPS)-challenged mice with or without OM85 pretreatment vs. control pregnant mice. Molecular drivers of gene coexpression networks in decidua of (**a**) LPS-challenged vs. control pregnant mice; (**b**) OM85-pretreated LPS-challenged vs. control pregnant mice. Molecular drivers highlighted in red denote activation and blue indicates inhibition.
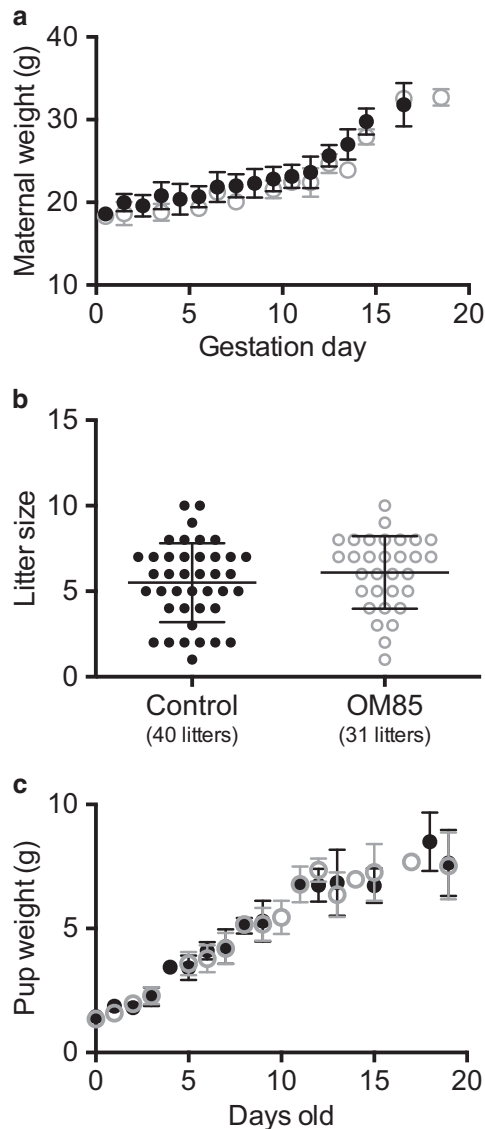
Figure 8 OM85 treatment did not alter normal pregnancy outcomes. Timed mated female mice treated with OM85 or naive/vehicle-treated controls were followed through pregnancy. (**a**) Maternal weight trajectory during pregnancy (● control $n = 26$ pregnancies, ○ OM85 $n = 13$ pregnancies), (**b**) litter size, and (**c**) pup weight trajectory from birth until weaning (control $n = 11$ litters, OM85 $n = 19$ litters) were measured. Data displayed as mean ± s.d., number of pups or litters shown in parentheses; no significant differences were found by unpaired t-test.

between cell surface vs. intracellular TLR4/LPS signaling in target cells, and this possibility is amenable to testing.

The mode of action of OM85 parallels the concepts of trained immunity, a term that describes the augmentation of innate immune function following a stimulus not specific to the original stimulus.[32,40,41] Further examples of the latter include protection against unrelated infectious diseases through vaccination and the seminal studies that have described striking protective effects of environmental microbial exposure via inhalation and dietary intake during pregnancy through living/working in a traditional European farming environment, on (*inter alia*) allergy and asthma development in offspring.[42,43]

LPS exposure of pregnant mice induces high levels of inflammatory cytokine/chemokine production (**Figure 4**) accompanied by the recruitment of anti-inflammatory immune cell populations (Tregs and MDSCs; **Figure 3**) in two of the three gestational tissues tested. Both mediator production and immune cell recruitment were attenuated in OM85-pretreated mice, consistent with reduction of the local inflammatory burden. An additional feature of the LPS response was the depletion of resident cDCs in gestational tissues (**Figure 3a,b**) which, in common with other inflammatory challenge models,[44,45] likely involves stimulation of their migration to draining lymph nodes in response to inflammatory triggers (**Figure 3d**). This depletion was blocked in OM85-pretreated mice (**Figure 3a,b**) suggesting that reducing the proinflammatory signature prevents egress of resident DC, or promotes recruitment of fresh cDC precursors to replace the LPS-responsive emigrant population, and moreover enhances their activation upon arrival (**Supplementary Figure 7a–c**). In this regard, it is noteworthy that LPS exposure additionally triggered local infiltration by pDCs, which are important components of the innate immune response to pathogens,[46,47] and this recruitment was also markedly enhanced in OM85-pretreated mice (**Figure 3a,c**), suggesting that the overall DC precursor compartment represents a major OM85 target.

With respect to the associated cellular effector mechanisms, it is pertinent to note that the cDC and pDC populations in gestational tissues identified above as prominent OM85 targets are both recognized as key contributors to regulation of pathogen-specific immunity.[46,48,49] Moreover, upregulation of cDC function has previously been identified in association with OM85-mediated stimulation of protective antibody responses against respiratory pathogens in a mouse model.[50]

In conclusion, this study provides experimental proof of concept that oral treatment during pregnancy with the microbial-derived agent OM85 provides broad-spectrum protection against the systemic effects of inflammatory responses triggered by both bacterial and viral agents, in particular against responses in gestational tissues that are associated with fetal loss and/or growth restriction. These findings suggest that existing microbial-derived therapeutics with immunomodulatory properties and proven safety records may provide novel therapeutic options for protection against the toxic effects of infections during pregnancy. Moreover, they point towards opportunities for the development of defined molecular entities with comparable modes of action, for therapeutic use in this and related clinical contexts.

METHODS

Animals. Specific pathogen-free BALB/c mice were obtained from the Animal Resources Centre (Perth, WA, Australia). Female mice were used for timed mating only between 8 and 12 weeks of age. Male studs were used from 8 weeks of age and retired at 36 weeks of age. All the mice were housed under specific pathogen-free conditions at the Telethon Kids Bioresources Facility, with food and water *ad libitum* and a 12 h light/dark cycle. All the experiments were approved by the Telethon Kids Animal Ethics Committee, and strictly conducted

according to the NHMRC guidelines for the use of animals for scientific research.

Time mated pregnancy. Male stud mice were caged individually. Up to two female mice were placed in a male cage overnight and the following morning females were separated from the males and checked for vaginal plugs as evidence of mating. The females were designated gestational day (GD) 0.5 on the day of vaginal plug detection and housed in groups of 5–10 until commencement of treatments. Females not pregnant after plug detection were killed.

Treatment protocols

OM85 treatment. OM85 was administered orally via pipette at a dose of 400 mg kg^{-1} body weight in phosphate-buffered saline (PBS) per day. In the Influenza A virus infection model, time mated females were administered OM85 daily for 9 days from GD0.5 until the day of PR8 infection (**Supplementary Figure 1**). The control mice were left untreated, or were administered the vehicle orally on the same treatment regimens. In the LPS challenge model, pregnant female mice were administered OM85 daily from GD9.5 until LPS challenge on GD16.5, or delivery (**Supplementary Figure 4**). All the treatments were performed using a single batch of OM85, supplied by OM Pharma (Geneva, Switzerland).

Influenza infection. The mouse-adapted Influenza A/PR/8/34 virus was from the American Type Tissue Culture Collection and prepared in allantoic fluid of 9-day old embryonated hen eggs. Stock virus was sub-passaged through Madin–Darby canine kidney cells in Dulbecco's modified Eagle's medium (DMEM; Gibco, Sydney, Australia), harvested as tissue culture supernatant and viral titers determined by cytopathic effects on Madin–Darby canine kidney cells and expressed as the mean log10 tissue culture infective dose that kills 50% of the cells (TCID50) over a 5-day incubation period.[16] Non-pregnant control and GD9.5 pregnant mice were inoculated intranasally under light inhalation isoflurane anesthesia with a dose of 20 TCID$_{50}$ of PR8, diluted in PBS, in a total volume of 25 µl. The mice were monitored daily for weight loss and clinical score (as below).[16] At the peak of disease (GD17.5), BAL and tissues were collected and fetal/placental weights were recorded (**Supplementary Figure 1**).

Viral load post infection was measured in lung homogenate by real-time quantitative PCR. Lungs were homogenized in PBS (10% w/v) and RNA was extracted using TRIzol (Ambion, Life Technologies, Mulgrave, VIC, Australia) and RNeasy MiniElute kit (Qiagen Gmbh, Hilden, Germany). The complementary DNA (cDNA) was prepared with Quantitect Reverse Transcription Kit (Qiagen) and PR8 Polymerase A was detected using Quantifast SYBR Green PCR master mix (Qiagen) and the following primers, 5′-CGGTCC AAATTCCTGCTGA-3′ and 5′-CATTGGGGTTCCTTCCATCCA-3′ (Sigma-Aldrich, St Louis, MO, USA). Copy numbers were calculated using a standard curve of known amounts of amplified cDNA.

LPS challenge. Female mice at gestational day 16.5 were administered 10 µg of LPS (*Salmonella typhimurium*, Sigma-Aldrich) in 200 µl of PBS via intraperitoneal injection as previously described.[21] The controls were administered 200 µl of PBS intraperitoneally. Twenty-four hours later at gestational day (GD) 17.5, an autopsy was conducted and tissues and serum collected for further analysis (**Supplementary Figure 4**).

Animal monitoring and clinical assessments. The mice were weighed daily during the acute period of infection (d0 to autopsy day). Clinical disease scores were also assessed according to the following criteria:

Score 0—normal appearance, healthy and active.

Score 1—barely ruffled fur, mildly/intermittent hunched appearance, and otherwise healthy.

Score 2—moderately ruffled fur, elevated respiratory rate, hunched appearance with a crab-like gait, intermittent stillness, and reduction of curious behavior.

Score 3 - Ruffled fur, labored breathing, hunched appearance with a crab-like gait, and unresponsive to stimuli.

Tissue dissection. At gestational day 17.5, the tissues were collected only from implantation sites from overtly normal fetuses, dead fetuses were excluded. Following the killing of the pregnant mouse, the placentas were peeled/blunt dissected from the maternal tissue. Then, using small scissors, a portion of mesometrial uterus approximately 3 mm^2 was dissected, which was full thickness, and therefore included the decidua, but also the residual lymphoid aggregate of pregnancy and some myometrium, this we have termed 'decidua'. The remaining anti-mesometrial uterus was also collected, which was also full thickness, and but was primarily myometrium, this we have termed 'uterus'. The terms 'decidua' and 'uterus' have been used throughout for simplicity for the general reader. Tissue harvesting was performed consistently across all the experimental groups.

Cell preparations. Single cell suspensions of uterus, decidua, placenta, and para-aortic lymph nodes were prepared by enzymatic digestion using methodology as previously described.[16] Briefly, following dissection, the tissues were sliced into small pieces, resuspended in GKN (11 mM D-glucose, 5.5 mM KCl, 137 mM NaCl, 25 mM Na_2HPO_4) + 10% FCS (fetal calf serum; Serana, Bunbury, WA, Australia) containing collagenase IV (Worthington Biochemical Corporation, Lakewood, NJ, USA) and DNase (Sigma-Aldrich) and incubated at 37 °C with gentle agitation as follows. Uterus: 1.5 mg ml^{-1} collagenase IV and 0.2 mg ml^{-1} DNase for 60 min; decidua and placenta: 0.75 mg ml^{-1} of collagenase and 0.1 mg ml^{-1} of DNase for 60 min; and para-aortic lymph node: 0.75 mg ml^{-1} of collagenase and 0.1 mg ml^{-1} of DNase for 30 min. Following digestion, the tissues were finally redispersed via pipetting, and debris removed by passing suspensions through cotton wool columns. The cells were pelleted and resuspended in PBS with 0.1% bovine serum albumin (Bovagen Biologicals, VIC, Australia), prepared for total cell counts or other assays as below. For the placenta, the digested preparation was resuspended in GKN + 5% FCS and further enriched for leukocytes via Histopaque (Sigma-Aldrich) gradient enrichment as per the manufacturer's instructions.

Broncho-alveolar lavage fluid was harvested by slowly infusing and withdrawing 1 ml PBS containing 1 mg ml^{-1} BSA from the lungs three times. The cells were pelleted and prepared for total cell counts and differential cell counts as previously described.[16] Briefly, the percentage of each cell type as identified by Diff Quik stain (macrophage, neutrophil, eosinophil, lymphocyte) was calculated as a proportion of at least 300 counted cells, and this figure used to derive total numbers of each subset based on the total broncho-alveolar lavage fluid cell count.

Flow cytometry. Immunostaining of viable single cells was conducted as previously described.[16] Two panels of monoclonal antibodies (**Supplementary Table 2**) were developed to identify leukocytes of myeloid (including CD45, I-A/I-E, F480, Ly6G/C, B220, CD11c, CD11b, CD103, CD8, CD40, CD86, and NKp46 (BD Pharmingen, San Jose, CA, USA or eBiosciences, San Diego, CA, USA) and lymphoid (using CD45, CD3, CD4, CD8, CD19, CD25, CD69, Ki67, and FoxP3 as per **Supplementary Table 2**; BD Pharmingen or BioLegend, San Diego, CA, USA) lineages, and subsets therein.[26,51–54] Intracellular staining for FoxP3 was conducted using the eBiosciences FoxP3 intracellular staining buffer set. The data were collected on a four-laser LSRFortessa flow cytometer (BD Biosciences, San Jose, CA, USA), and analyzed using FlowJo software (Version 10.0.7, Tree Star, Sanford, CA, USA).

viSNE methods. Placenta sample FCS files, with software compensation applied, were uploaded to Cytobank software (Cytobank Mountain View, CA, USA), and analyzed using established methods.[55,56] The software transformed the data to arcsinh scales with cofactors ranging from 20 to 2,500. Equal cell numbers were analyzed from each FCS file. The antibodies listed as per **Supplementary Table 2** for dendritic cell and subset identification were used to create

viSNE maps using a total of 22,570 cells per sample. The antibodies for T-cell and Treg identification were used to create viSNE maps using a total of 17,829 cells per sample.

Multiplex cytokine analysis on maternal serum. Maternal blood was collected by cardiac puncture during autopsy on GD 17.5. Serum was assayed for cytokines using a Bio-Plex Pro mouse cytokine 23plex kit (Bio-Rad Laboratories, Hercules, CA, USA), following the manufacturer's instructions. IL-1α, IL-1β, IL-2, IL-3, IL-4, IL-5, IL-6, IL-9, IL-10, IL-12p40, IL-12p70, IL-13, IL-17, Eotaxin, G-CSF, GM-CSF, IFN-γ, KC, MCP-1, MIP-1α, MIP-1β, RANTES, and TNF-α were included in this assay.

Multiplex cytokine analysis on gestational tissue samples
Tissue collection. The uterus and placenta samples were collected at autopsy on GD17.5. A randomly selected longitudinal quarter of the uterus and a quarter of each placenta was snap frozen in liquid nitrogen for protein extraction.

Tissue preparation and cytokine analysis. The uterus and placenta tissue samples were processed using a Bio-Plex Cell Lysis Kit (Bio-Rad Laboratories), following the manufacturer's instructions. Briefly, the samples were homogenized with 500 μl of lysing solution and frozen overnight at $-80\,^{\circ}$C. The following day, the samples were sonicated, centrifuged at 4,500 g for 4 min, and the supernatant collected. The protein content of the supernatant was determined using a DC Protein Assay (Bio-Rad Laboratories). A total 900 μg ml^{-1} of protein was then assayed for cytokines using a separate Bio-Plex Pro mouse cytokine 23 plex kit (Bio-Rad Laboratories), following the manufacturer's instructions.

RNA isolation and transcriptome profiling (RNA-Seq)
Tissue collection. The uterus, deciduas, and placenta samples were collected at autopsy on GD17.5. The entire decidua and a randomly selected longitudinal quarter of the uterus was placed in RNAlater (Ambion) overnight at 4 °C. The tissues were then transferred to a fresh tube and frozen at $-80\,^{\circ}$C for RNA extraction and transcriptome profiling.

Tissue preparation, RNA extraction, and transcriptome profiling. Decidua and uterus tissue samples were homogenized utilizing a rotor-stator homogenizer (Qiagen), and total RNA was extracted using TRIzol (Ambion) followed by RNeasy MinElute (Qiagen). The integrity of the RNA was assessed on the Bioanalyzer (RIN: 9.4 ± 0.2 (mean ± s.d.)). Total RNA samples were shipped to AGRF for library preparation (TruSeq Stranded mRNA Library Prep Kit, Illumina Inc, San Diego, CA) and sequencing (Illumina HiSeq2500, 50bp single-end reads, v4 chemistry, $n = 48$). Twenty-five million reads were generated per sample. The raw sequencing data are available from GEO (accession; GSE85414).

RNA-Seq data analysis. The RNA-Seq data were analyzed in the R environment for statistical computing. The quality of the sequencing data was assessed with the Bioconductor package Rqc. Sequencing reads were aligned to the reference genome (mm10) using Subread, and summarized at the gene level using featureCounts.[57] Genes with less than 500 total counts across the data were removed from the analysis. Sample QC was performed by examining Relative Log Expression and Principal Component Analysis plots, and outlier samples were removed from the analysis. The DEGs were identified using negative binomial models in edgeR, with FDR control for multiple testing.[58] The InnateDB database was utilized for pathways analysis.[59] Molecular drivers of DEGs and networks were identified using Upstream Regulator Analysis.[30] Upstream regulators with absolute activation Z-scores <2.0 were filtered out of the analysis, and were ranked by their overlap P value. A coexpression network was constructed from the RNA-Seq data using the WGCNA algorithm.[28,29] A separate network was constructed for each tissue

(decidua, uterus). Before network analysis, the count data were transformed using the varianceStabilizingTransformation algorithm from the DESeq2 package.[58] Network analysis was restricted to the top ~5,000 most variable genes, and these were identified using the varianceBasedfilter algorithm from the Bioconductor package DCGL. The modules identified by WGCNA were examined for enrichment of DEGs by calculating a median FDR for each module that was based on the gene-level statistics derived from the edgeR analysis.

Statistical analysis. Statistical analyses were performed using GraphPad Prism software (version 6.0 g for Mac OSX, La Jolla, CA, USA). Unpaired *t*-tests, one-way and two-way analyses of variance followed by Bonferroni multiple comparisons tests were used as indicated in the figure legends. The figures include the number of animals or litters per group.

PCA was performed using the FactoMineR R package.[19] Parameters used in the PCA included: clinical score, maternal weight, fetal weight, BAL cells, and viral copy number (**Supplementary Table 1**). The first two dimensions (PCA 1 and PCA 2) accounted for 79% of the variability between the samples.

AUTHOR CONTRIBUTIONS
A.B., P.G.H., and D.H.S. designed and supervised the study. N.M.S., J.F.L.-J., K.T.M. and M.S. performed the experiments. N.M.S., J.F.L.-J., A.C.J., K.T.M., N.M.T., J.L., A.B., and D.H.S. analyzed the data. S.A.R., S.L.P., C.P. contributed to the project design, methodology, and discussions on data interpretation. A.B., P.G.H., and D.H.S. wrote the manuscript. All the authors reviewed the final manuscript.

REFERENCES
1. Lapinsky, S.E. Obstetric infections. *Crit. Care Clin.* **29**, 509–520 (2013).
2. Sappenfield, E., Jamieson, D.J. & Kourtis, A.P. Pregnancy and susceptibility to infectious diseases. *Infect. Dis. Obstet. Gynecol.* **2013**, 752852 (2013).
3. Kemp, M.W. Preterm birth, intrauterine infection, and fetal inflammation. *Front. Immunol.* **5**, 574 (2014).
4. Romero, R., Dey, S.K. & Fisher, S.J. Preterm labor: one syndrome, many causes. *Science* **345**, 760–765 (2014).
5. Arck, P.C. & Hecher, K. Fetomaternal immune cross-talk and its consequences for maternal and offspring's health. *Nat. Med.* **19**, 548–556 (2013).
6. Barker, D.J. & Thornburg, K.L. The obstetric origins of health for a lifetime. *Clin. Obstet. Gynecol.* **56**, 511–519 (2013).
7. Meijer, W.J., van Noortwijk, A.G., Bruinse, H.W. & Wensing, A.M. Influenza virus infection in pregnancy: a review. *Acta Obstet. Gynecol. Scand.* **94**, 797–819 (2015).

8. Luan, H. *et al.* OM85-BV induced the productions of IL-1beta, IL-6, and TNF-alpha via TLR4- and TLR2-mediated ERK1/2/NF-kappaB pathway in RAW264.7 cells. *J. Interferon Cytokine Res.* **34**, 526–536 (2014).

9. Parola, C. *et al.* Selective activation of human dendritic cells by OM-85 through a NF-kB and MAPK dependent pathway. *PLoS One* **8**, e82867 (2013).

10. Schaad, U.B. OM-85 BV, an immunostimulant in pediatric recurrent respiratory tract infections: a systematic review. *World J. Pediatr.* **6**, 5–12 (2010).

11. Weinberger, M. Can we prevent exacerbations of asthma caused by common cold viruses?. *J. Allergy Clin. Immunol.* **126**, 770–771 (2010).

12. Emmerich, B., Emslander, H.P., Pachmann, K., Hallek, M., Milatovic, D. & Busch, R. Local immunity in patients with chronic bronchitis and the effects of a bacterial extract, Broncho-Vaxom, on T lymphocytes, macrophages, gamma-interferon and secretory immunoglobulin A in bronchoalveolar lavage fluid and other variables. *Respiration* **57**, 90–99 (1990).

13. Collet, J.P. *et al.* Stimulation of nonspecific immunity to reduce the risk of recurrent infections in children attending day-care centers. The Epicreche Research Group. *Pediatr. Infect. Dis. J.* **12**, 648–652 (1993).

14. Razi, C.H. *et al.* The immunostimulant OM-85 BV prevents wheezing attacks in preschool children. *J. Allergy Clin. Immunol.* **126**, 763–769 (2010).

15. Soler, M., Mutterlein, R. & Cozma, G. Double-blind study of OM-85 in patients with chronic bronchitis or mild chronic obstructive pulmonary disease. *Respiration* **74**, 26–32 (2007).

16. Strickland, D.H. *et al.* Persistent and compartmentalised disruption of dendritic cell subpopulations in the lung following influenza A virus infection. *PLoS One* **9**, e111520 (2014).

17. Raj, R.S., Bonney, E.A. & Phillippe, M. Influenza, immune system, and pregnancy. *Reprod. Sci.* **21**, 1434–1451 (2014).

18. Rasmussen, S.A., Jamieson, D.J. & Uyeki, T.M. Effects of influenza on pregnant women and infants. *Am. J. Obstet. Gynecol.* **207** (3 Suppl), S3–S8 (2012).

19. Lê, S., Josse, J. & Husson, F. *FactoMineR: an R package for multivariate analysis* **25**, 18 (2008).

20. Nadeau-Vallee, M. *et al.* Novel noncompetitive IL-1 receptor-biased ligand prevents infection- and inflammation-induced preterm birth. *J. Immunol.* **195**, 3402–3415 (2015).

21. Robertson, S.A., Skinner, R.J. & Care, A.S. Essential role for IL-10 in resistance to lipopolysaccharide-induced preterm labor in mice. *J. Immunol.* **177**, 4888–4896 (2006).

22. Cappelletti, M., Della Bella, S., Ferrazzi, E., Mavilio, D. & Divanovic, S. Inflammation and preterm birth. *J. Leukoc. Biol.* **99**, 67–78 (2016).

23. Erlebacher, A. Immunology of the maternal-fetal interface. *Annu. Rev. Immunol.* **31**, 387–411 (2013).

24. Robertson, S.A., Petroff, M.G. & Hunt, J.S. Immunology of pregnancy. In: *Knobil and Neill's Physiology of Reproduction*, 4th edn (Plant, T.M., Zeleznik, A.J., eds) 1835–1874 (Elsevier, Oxford, UK, 2015).

25. Tagliani, E. & Erlebacher, A. Dendritic cell function at the maternal-fetal interface. *Expert Rev. Clin. Immunol.* **7**, 593–602 (2011).

26. Zhao, H., Kalish, F., Schulz, S., Yang, Y., Wong, R.J. & Stevenson, D.K. Unique roles of infiltrating myeloid cells in the murine uterus during early to midpregnancy. *J. Immunol.* **194**, 3713–3722 (2015).

27. Collins, M.K., Tay, C.S. & Erlebacher, A. Dendritic cell entrapment within the pregnant uterus inhibits immune surveillance of the maternal/fetal interface in mice. *J. Clin. Invest.* **119**, 2062–2073 (2009).

28. Bosco, A., McKenna, K.L., Firth, M.J., Sly, P.D. & Holt, P.G. A network modeling approach to analysis of the Th2 memory responses underlying human atopic disease. *J. Immunol.* **182**, 6011–6021 (2009).

29. Langfelder, P. & Horvath, S. WGCNA: an R package for weighted correlation network analysis. *BMC Bioinformatics* **9**, 559 (2008).

30. Krämer, A., Green, J., Pollard, J. Jr & Tugendreich, S. Causal analysis approaches in ingenuity pathway analysis. *Bioinformatics* **30**, 523–530 (2014).

31. Pazos, M., Sperling, R.S., Moran, T.M. & Kraus, T.A. The influence of pregnancy on systemic immunity. *Immunol. Res.* **54**, 254–261 (2012).

32. Levy, O. & Wynn, J.L. A prime time for trained immunity: innate immune memory in newborns and infants. *Neonatology* **105**, 136–141 (2014).

33. Meissner, H.C. Viral bronchiolitis in children. *N. Engl. J. Med.* **374**, 62–72 (2016).

34. Hacker, H. *et al.* Specificity in Toll-like receptor signalling through distinct effector functions of TRAF3 and TRAF6. *Nature* **439**, 204–207 (2006).

35. Kagan, J.C., Su, T., Horng, T., Chow, A., Akira, S. & Medzhitov, R. TRAM couples endocytosis of Toll-like receptor 4 to the induction of interferon-beta. *Nat. Immunol.* **9**, 361–368 (2008).

36. Parker, D. & Prince, A. Type I interferon response to extracellular bacteria in the airway epithelium. *Trends Immunol.* **32**, 582–588 (2011).

37. Blank, V., Hirsch, E., Challis, J.R., Romero, R. & Lye, S.J. Cytokine signaling, inflammation, innate immunity and preterm labour - a workshop report. *Placenta* **29** (Suppl A), S102–S104 (2008).

38. Challis, J.R., Lockwood, C.J., Myatt, L., Norman, J.E., Strauss, J.F. 3rd & Petraglia, F. Inflammation and pregnancy. *Reprod. Sci.* **16**, 206–215 (2009).

39. Husebye, H. *et al.* Endocytic pathways regulate Toll-like receptor 4 signaling and link innate and adaptive immunity. *EMBO J.* **25**, 683–692 (2006).

40. van der Meer, J.W., Joosten, L.A., Riksen, N. & Netea, M.G. Trained immunity: a smart way to enhance innate immune defence. *Mol. Immunol.* **68**, 40–44 (2015).

41. Kleinnijenhuis, J. *et al.* BCG-induced trained immunity in NK cells: role for non-specific protection to infection. *Clin. Immunol.* **155**, 213–219 (2014).

42. von Mutius, E. & Radon, K. Living on a farm: impact on asthma induction and clinical course. *Immunol. Allergy Clin. North Am.* **28**, 631–647 (2008).

43. von Mutius, E. The microbial environment and its influence on asthma prevention in early life. *J. Allergy Clin. Immunol.* **137**, 680–689 (2016).

44. Jahnsen, F.L. *et al.* Accelerated antigen sampling and transport by airway mucosal dendritic cells following inhalation of a bacterial stimulus *J. Immunol.* **177**, 5861–5867 (2006).

45. Platt, A.M. & Randolph, G.J. Dendritic cell migration through the lymphatic vasculature to lymph nodes. *Adv. Immunol.* **120**, 51–68 (2013).

46. Asselin-Paturel, C. *et al.* Type I interferon dependence of plasmacytoid dendritic cell activation and migration. *J. Exp. Med.* **201**, 1157–1167 (2005).

47. Dai, J., Megjugorac, N.J., Amrute, S.B. & Fitzgerald-Bocarsly, P. Regulation of IFN regulatory factor-7 and IFN-alpha production by enveloped virus and lipopolysaccharide in human plasmacytoid dendritic cells. *J. Immunol.* **173**, 1535–1548 (2004).

48. Amit, I. *et al.* Unbiased reconstruction of a mammalian transcriptional network mediating pathogen responses. *Science* **326**, 257–263 (2009).

49. Bogdan, C., Mattner, J & Schleicher, U. The role of type I interferons in non-viral infections. *Immunol. Rev.* **202**, 33–48 (2004).

50. Pasquali, C. *et al.* Enhanced mucosal antibody production and protection against respiratory infections following an orally administered bacterial extract. *Front. Med.* **1**, 41 (2014).

51. Bizargity, P. & Bonney, E.A. Dendritic cells: a family portrait at mid-gestation. *Immunology* **126**, 565–578 (2009).

52. Gomez-Lopez, N., Olson, D.M. & Robertson, S.A. Interleukin-6 controls uterine Th9 cells and CD8(+) T regulatory cells to accelerate parturition in mice. *Immunol. Cell Biol.* **94**, 79–89 (2016).

53. Merad, M., Sathe, P., Helft, J., Miller, J. & Mortha, A. The dendritic cell lineage: ontogeny and function of dendritic cells and their subsets in the steady state and the inflamed setting. *Annu. Rev. Immunol.* **31**, 563–604 (2013).

54. Segura, E. & Amigorena, S. Inflammatory dendritic cells in mice and humans. *Trends Immunol.* **34**, 440–445 (2013).

55. Diggins, K.E., Ferrell, P.B. Jr & Irish, J.M. Methods for discovery and characterization of cell subsets in high dimensional mass cytometry data. *Methods* **82**, 55–63 (2015).

56. Kotecha, N., Krutzik, P.O. & Irish, J.M. Web-based analysis and publication of flow cytometry experiments. *Curr. Protoc. Cytom.* **Chapter 10**, Unit10.17 (2010).

57. Liao, Y., Smyth, G.K. & Shi, W. The Subread aligner: fast, accurate and scalable read mapping by seed-and-vote. *Nucleic Acids Res.* **41**, e108 (2013).

58. Anders, S. *et al.* Count-based differential expression analysis of RNA sequencing data using R and Bioconductor. *Nat. Protoc.* **8**, 1765–1786 (2013).

59. Lynn, D.J. *et al.* InnateDB: facilitating systems-level analyses of the mammalian innate immune response. *Mol. Syst. Biol.* **4**, 218 (2008).